

# Unusual swelling of a polymer in a bacterial bath

A. Kaiser<sup>1,\*</sup> and H. Löwen<sup>1</sup>

<sup>1</sup>*Institut für Theoretische Physik II: Weiche Materie,  
Heinrich-Heine-Universität Düsseldorf, Universitätsstraße 1, D-40225 Düsseldorf, Germany*  
(Dated: April 4, 2024)

The equilibrium structure and dynamics of a single polymer chain in a thermal solvent is by now well-understood in terms of scaling laws. Here we consider a polymer in a bacterial bath, i.e. in a solvent consisting of active particles which bring in nonequilibrium fluctuations. Using computer simulations of a self-avoiding polymer chain in two dimensions which is exposed to a dilute bath of active particles, we show that the Flory-scaling exponent is unaffected by the bath activity provided the chain is very long. Conversely, for shorter chains, there is a nontrivial coupling between the bacteria intruding into the chain which may stiffen and expand the chain in a nonuniversal way. As a function of the molecular weight, the swelling first scales faster than described by the Flory exponent, then an unusual plateau-like behaviour is reached and finally a crossover to the universal Flory behaviour is observed. As a function of bacterial activity, the chain end-to-end distance exhibits a pronounced non-monotonicity. Moreover, the mean-square displacement of the center of mass of the chain shows a ballistic behaviour at intermediate times as induced by the active solvent. Our predictions are verifiable in two-dimensional bacterial suspensions and for colloidal model chains exposed to artificial colloidal microswimmers.

PACS numbers: 61.25.he, 82.70.Dd, 61.30.Pq, 87.15.A-

## I. INTRODUCTION

The physics of polymer chains in a thermalized bath is governed by scaling laws. One of the most fundamental scaling relates the typical extension of a polymer chain  $R$  to its molecular weight  $N$  culminating in the traditional Flory exponent  $\nu$ , such that  $R \propto N^\nu$  [1, 2] for very large  $N$ . While  $\nu = 1/2$  for a Gaussian chain, a self-avoiding chain exhibits a Flory exponent  $\nu > 1/2$  which depends on the spatial dimensions  $d$ , we have  $\nu = 0.588 \approx 3/5$  in three and  $\nu = 3/4$  in two dimensions [3]. Similar scaling laws apply to the polymer dynamics where hydrodynamic interactions between the monomer play a crucial role [2]. It is important to note that these basic considerations are designed for equilibrium situations, i.e. the solvent is a thermal bath at temperature  $T$  and the chain is not exposed to external fields.

In this paper we consider a polymer chain in a bacterial (or active) bath which consists of swimming particles or bacteria. The collisions of the bacteria with the chain lead to nonequilibrium (non-thermal) fluctuations of the chain which may result in new phenomena of chain stretching and compaction different from equilibrium solvents. Active matter itself has been intensely explored over the last years, both for living systems as bacteria [4], spermatozoa [5] and mammals [6, 7] or is system of artificial microswimmers [8–13] with various propulsion mechanisms [14–17] and a plethora of nonequilibrium pattern formation phenomena were discovered [18–33]. At fixed system boundaries active system show distinct clustering and trapping behaviour [34–45] and can be exploited to

steer the motion of microrotors and microcarriers [46–48] of fixed shape.

Here we link the field of microswimmers to polymer physics and consider a single polymer chain in a bacterial bath (or an active solvent). The motivation to do so is threefold: first, from a fundamental point of view, there is a need to understand how polymer scaling laws are affected by non-bulk or nonequilibrium situations [49–52]. An active solvent which is intrinsically in nonequilibrium is one of basic cases which put the scaling laws into questions. Second, the collective behaviour of microswimmers has been studied at moving boundaries [46, 53, 54] but all of which were of fixed shape. Bacteria and active particles near flexible boundaries have not yet been explored systematically and it is interesting to understand how clustering and trapping phenomena are modified for flexible boundaries [55]. Our case of a flexible polymer chain is therefore one of the simplest key examples to proceed along this important direction. Third, in general, the set-up we are proposing is realizable in experiments and relevant for biological systems where swarms of bacteria are moving close to flexible objects like at water-air interfaces [56–61]. Our two-dimensional model can indeed be realized e.g. by inserting long polymers into two-dimensional *Bacillus subtilis* suspensions [19, 24, 46]. Another complementary realization is by exposing colloidal model chains [62] to artificial colloidal microswimmers [11, 63, 64].

We use computer simulations of a self-avoiding polymer chain in two dimensions which is exposed to a dilute bath of active particles. As a result, we show that the Flory-scaling exponent  $\nu = 3/4$  is unaffected by the bath activity provided the chain is very long. For shorter chains, there is a nontrivial coupling between the bacteria intruding into the chain which stiffen

---

\* kaiser@thphy.uni-duesseldorf.de

and expand the chain. As a function of the molecular weight, the swelling first scales faster than described by the Flory exponent until a plateau-like behaviour with a slight non-monotonicity is reached. This is nonuniversal behaviour which reminds to the swelling of polymers in quenched disordered where similar nonmonotonicities have been observed [65, 66] which have, however, a different physical origin. Finally, for large molecular weights, a crossover to the universal Flory behaviour is observed. Moreover, as a function of bacterial activity, the chain end-to-end distance shows a pronounced non-monotonicity. The dynamical correlations exhibit a diffusive behaviour for very short and long times in qualitative accordance with an equilibrated polymer, while an intermediate ballistic regime can be found in the mean-square displacement of the center of mass of the chain induced by the active solvent.

This paper is organized as follows: we introduce our model and our computer simulation technique in section II. Various results on the statistics of polymer structure in a bacterial bath are presented in section III while the polymer dynamics is discussed in section IV. Finally we conclude and give an outlook in section V.

## II. MODEL

We study the statistics of a polymer chain, modeled as a sequence of  $N$  coarse-grained spring beads, in a bacterial bath, composed of spherical swimmers in two dimensions, see Fig. 1. For simplicity, interactions between the active particles and the chain as well as inter-chain interactions are modeled by the same repulsive WCA-potential

$$U_{\text{WCA}}(r) = 4\epsilon \left[ \left( \frac{\sigma}{r} \right)^{12} - \left( \frac{\sigma}{r} \right)^6 \right] + \epsilon, \quad (1)$$

for distances  $r < 2^{1/6}\sigma$ . Here the diameter of a bead and a disk-like swimmer is assumed to be equal and is denoted with  $\sigma$  and  $\epsilon = k_B T$  is the interaction strength. These quantities represent the length and energy units, while times are measured in  $\tau = \sigma^2/D_0$ , where  $D_0$  is the short-time diffusion constant of a single monomer.

Springs are introduced via a so-called FENE (finitely extensible nonlinear elastic) potential [67]

$$U_{\text{FENE}}(r_{ij}) = -\frac{1}{2}KR_0^2 \ln \left[ 1 - \left( \frac{r_{ij}}{R_0} \right)^2 \right], \quad (2)$$

with neighboring beads  $i, j$  and their distance  $r_{ij} = |\mathbf{r}_i - \mathbf{r}_j|$ . The spring constant is fixed to  $K = 27\epsilon/\sigma^2$  and the maximum allowed bond-length to  $R_0 = 1.5\sigma$ . These interactions ensure that for the parameters chosen the swimmers do not cross the polymer chain.

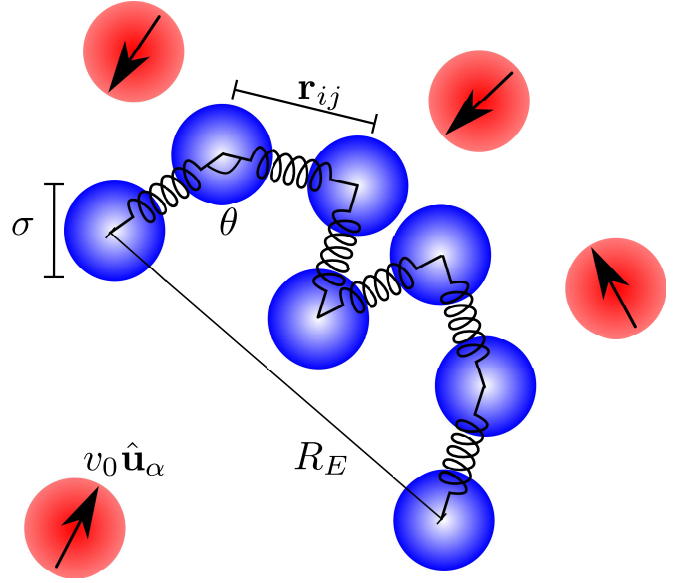


FIG. 1. Schematic sketch of the system for a chain with a low number  $N = 7$  of beads (blue) connected by springs with bond angle  $\theta$ . Furthermore the end-to-end distance  $R_E$  is indicated. The  $\alpha$ th self-propelled disk (red – bottom left) is driven along the marked orientation  $\hat{\mathbf{u}}_\alpha$  (black arrow) with a velocity  $v_0$ .

In our chosen units, the overdamped equation of motion of the  $i$ th bead located at position  $\mathbf{r}_i = [x_i(t), y_i(t)]$  is given by

$$\partial_t \mathbf{r}_i(t) = -\nabla_i U + \boldsymbol{\xi}_i \quad (3)$$

where  $\boldsymbol{\xi}_i$  is Gaussian white noise with zero mean and correlations  $\langle \boldsymbol{\xi}_i(t) \boldsymbol{\xi}_j(t') \rangle = 2D_0 \delta_{ij} \delta(t-t') \mathbb{1}$  with the unit tensor  $\mathbb{1}$ , and  $U$  is the total potential energy. The overdamped equation of motion for a swimmer  $\alpha$  is described through

$$\partial_t \mathbf{r}_\alpha(t) = -\nabla_\alpha U + v_0 \hat{\mathbf{u}}_\alpha(t) + \boldsymbol{\xi}_\alpha \quad (4)$$

where  $\boldsymbol{\xi}_\alpha$  is Gaussian white noise as before,  $U$  is the total potential interaction, and  $v_0$  is a self-propulsion velocity directed along  $\hat{\mathbf{u}}_\alpha = (\cos \varphi_\alpha, \sin \varphi_\alpha)$ , which will be given by the dimensionless Péclet number  $Pe = v_0 \sigma / D_0$ . The presence of  $v_0$  brings the system inherently into non-equilibrium. Finally, the orientation of the swimmer is coupled to the rotational Langevin equation

$$\partial_t \hat{\mathbf{u}}_\alpha(t) = \boldsymbol{\zeta}_\alpha \times \hat{\mathbf{u}}_\alpha(t). \quad (5)$$

Here  $\boldsymbol{\zeta}_\alpha$  is as well a Gaussian-distributed noise with zero mean and variance  $\langle \boldsymbol{\zeta}_\alpha(t) \boldsymbol{\zeta}_\beta(t') \rangle = 2D_r \delta_{\alpha\beta} \delta(t-t') \mathbb{1}$  and the corresponding rotational diffusion coefficient is  $D_r = 3D_0/\sigma$ .

Steric interactions between the active particles are modeled by a soft repulsive Yukawa potential. The total pair potential between a pair of disks  $\{\alpha, \beta\}$ , is given by

$$U_{\alpha\beta} = U_0 \frac{\exp(-r_{\alpha\beta}/\sigma)}{r_{\alpha\beta}}, \quad (6)$$

where the screening length corresponds to the disk diameter  $\sigma$  and  $r_{\alpha\beta} = |\mathbf{r}_\alpha - \mathbf{r}_\beta|$  is the distance between the swimmers, the prefactor is set to  $U_0 = 20\epsilon$ .

We perform Brownian dynamic simulations for various chain lengths  $1 \leq N \leq 1000$  ( $N = 1$  refers to the case of a single spherical tracer) using periodic boundary conditions in a square simulation domain with an area  $A = L_0^2$  where  $L_0 \sim N\sigma$  corresponds to the contour length of a linear chain in equilibrium. In integrating the Brownian dynamic equations of motion, we have used a finite time step  $10^{-7}\tau$ . The number of bacteria is determined by the dimensionless packing fraction

$$\phi = \frac{N_S \sigma^2}{4A}, \quad (7)$$

where  $N_S$  is the number of swimmers. We are interested in a dilute bacterial bath, so we chose  $\phi \leq 0.02$ , which is below the jamming transition for self-propelled disks [68]. Statistics are gathered for 20 to 50 independent simulation runs.

### III. RESULTS

As a key result, in Fig. 2 the dependence of the end-to-end distance on the molecular weight is shown on a double-logarithmic plot where the slope indicating the typical two-dimensional Flory scaling with  $\nu = 3/4$  is also indicated. For small chain lengths, the polymer swells stronger than Flory scaling which is obviously more pronounced for large activities  $Pe$ . The strong swelling results from events where a bacterium intrudes into the polymer chain stretching it, see inset of Fig. 2. Increasing the molecular weight  $N$  further results again in more coiling such that a plateau-like regime is reached, the associated molecular weight needed to reach the plateau depends on the Péclet number. Even a slight nonmonotonicity is compatible with the statistical uncertainties. Finally a crossover to the universal Flory behaviour of a self-avoiding chain is observed. This is expected since at very large scales only the statistics of self-avoidance should matter. In this limit, the presence of the bacteria are just providing some kind of higher effective temperature to the polymer such the typical entropically generated Flory exponent is obtained, compare to a similar finding in [69]. Clearly, the non-universal plateau-like behaviour is also found when the radius of gyration is plotted instead of the end-to-end distance, see again Fig. 2. In Fig. 2(b), the polymer extension is again shown versus the molecular weight  $N$  but is now scaled with its equilibrium value for vanishing activity at same  $N$ .

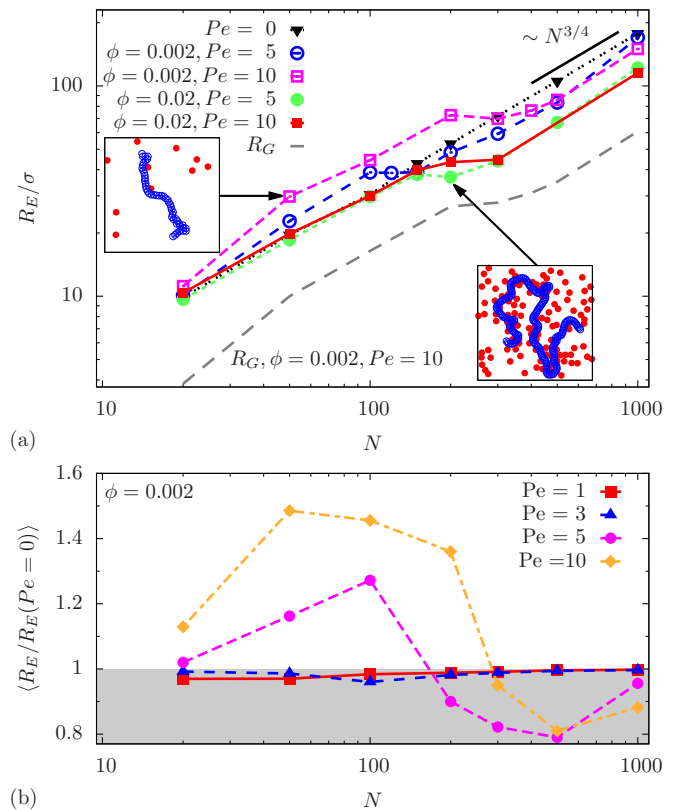


FIG. 2. (a) End-to-end distance  $R_E$  as a function of number of monomers  $N$  for different bacterial densities  $\phi$  and different self-propulsion strengths  $Pe$ . Line corresponds to the radius of gyration  $R_G$  of the polymer for the given parameters. (b) Relative end-to-end distance, now scaled with its value at vanishing Péclet number, versus molecular weight  $N$  for different Péclet numbers at  $\phi = 0.002$ .

By definition, this quantity is unity when  $Pe = 0$  but varies with increasing Péclet number. Interestingly, for this quantity there is a marked nonmonotonicity in  $N$  at intermediate Péclet numbers. For small  $N$ , the scaled end-to-end distance  $R_E/R_E(Pe = 0)$  is larger than unity quantifying the stretching effect by the bacteria sliding along the polymer chain. For larger  $N$ , the collisions of the bacteria with the polymer chain lead effectively to a compression as signalled by  $R_E/R_E(Pe = 0) < 1$ .

The distribution of the end-to-end distance is shown in Fig. 3(a) for various Péclet numbers for a fixed molecular weight  $N = 50$  revealing a broad peak which first shifts to the left and subsequently to the right for increasing  $Pe$ . For intermediate Péclet numbers the peak is pretty broad documenting the strong polymer fluctuations imprinted by the bacterial bath. The quantitative analysis of the shift is shown in Fig. 3(b) where the end-to-end distance in units of the contour length  $L_0$  is plotted versus Péclet number for various  $N$  and at fixed diluted  $\phi = 0.002$ . For fixed  $N$ , a nonmonotonic behaviour of  $R_E/L_0$  (or equivalently of  $R_E/\sigma$ ) is clearly revealed as a function of Péclet numbers. This can qualitatively understood as follows:

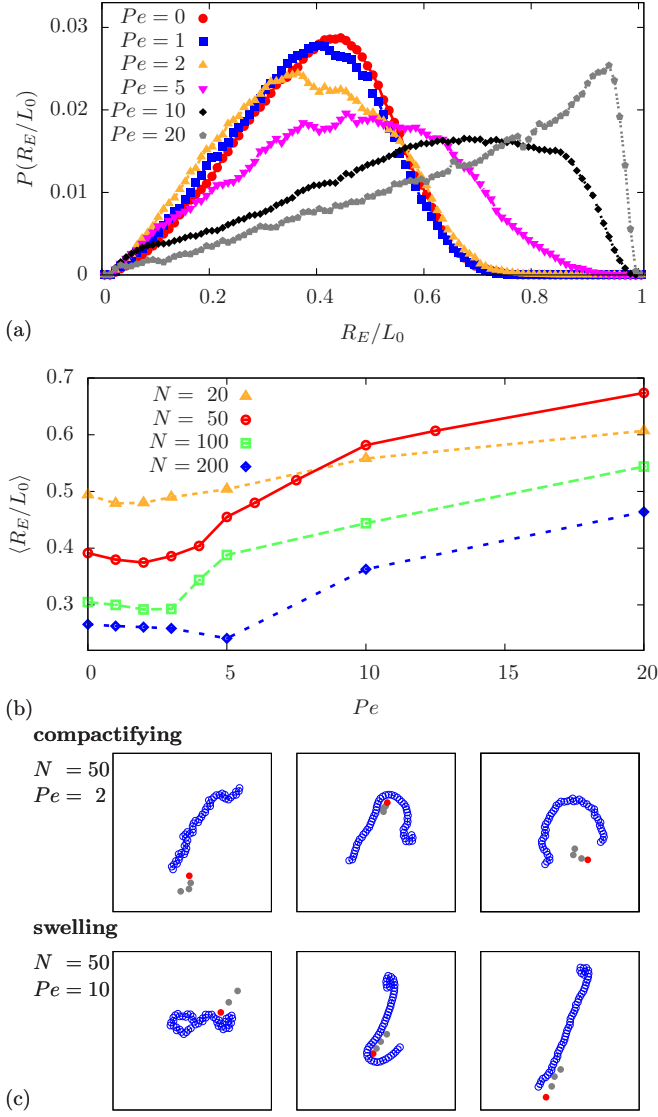


FIG. 3. (a) Probability distribution function of the reduced end-to-end distance  $R_E/L_0$  for various self-propulsion strengths  $Pe$  and fixed chain length  $N = 50$ . (b) Averaged reduced end-to-end distance  $\langle R_E/L_0 \rangle$  as a function of  $Pe$  for various chain lengths and end-to-end distance for various molecular weights  $N$ . (c) Time sequences showing the compactifying and the swelling of a polymer due to an active swimmer. Swimmer trajectories are indicated by its swimmer positions.

for small  $Pe$  a bacterium intrudes into the swollen chain and thus compactifying it, see also the snapshot series in Figure 3(c). The larger  $Pe$  becomes, the more is the bacterium able to really stretch the chain by sliding along it which then induces an increase in the averaged polymer extension. This scenario occurs over the whole range of molecular weight explored in this paper and is therefore quite general. The critical Péclet number for which the averaged polymer size is getting minimal increases with increasing molecular weight  $N$ , see Fig. 3(b).

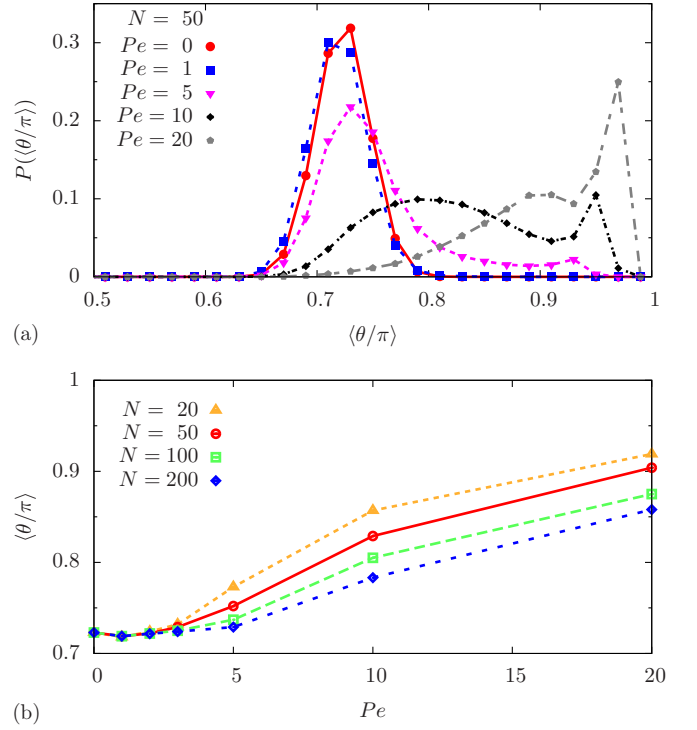


FIG. 4. (a) Probability distribution function of the averaged bond angle  $\langle \theta \rangle$  at fixed  $N = 50$  for various Péclet numbers  $Pe$ . (b) Averaged bond angle  $\theta$  versus self-propulsion strength  $Pe$  for various molecular weights  $N$ .

Finally we explore the impact of the intruding bacteria on the bond angle  $\theta$  of subsequent monomers along the chain in Fig. 4. The statistical distribution of  $\theta$ , as shown in Fig. 4(a), reveals a double peak of stretched parts of the chain where the bacteria are scratching along and a coiled part unaffected by the bacteria, see again Fig. 3(c). The average value  $\langle \theta \rangle$  increases with  $Pe$  reaching slowly the asymptotic value of  $\pi$  due to full chain stretching induced by a bacterium travelling along the polymer, see Fig. 4(b).

#### IV. POLYMER DYNAMICS

We finally turn to the influence of the bacterial bath on the polymers dynamics which is typically measured in terms of mean-square displacements. One may consider the latter for the end-monomer position  $\mathbf{r}_N$ , the end-to-end distance  $R_E$  itself, and the center of mass position  $\mathbf{r}$ .

Let us first recall the well-known scalings for a polymer in a thermal bath, corresponding to the case  $Pe = 0$ . In equilibrium, in the absence of hydrodynamic interactions, the mean square displacement of the *end-monomer* behaves as [70]

$$\langle (\Delta \mathbf{r}_N)^2 \rangle \sim t + \lambda(1 - \exp^{-t/\tau_p}), \quad (8)$$

for long times where  $\lambda$  is a constant coefficient and  $\tau_p$  a characteristic polymeric relaxation time. For very short times  $\langle(\Delta \mathbf{r}_N)^2\rangle$  is diffusive (i.e. linear in  $t$ ). The crossover behaviour from short to long times can be studied in terms of the logarithmic derivative which sets an effective time-dependent exponent as  $\gamma(t) = d \log \langle(\Delta \mathbf{r}_N)^2\rangle / d \log t$ . As a function of increasing time  $t$ , this exponent first decreases from 1 down to values of approximately 0.5 and then increases back to 1.

The mean-square displacement of the *end-to-end distance* in equilibrium is given for long times by [49]

$$\langle(\Delta R_E)^2\rangle \sim (1 - \exp^{-t/\tau_p}) \quad (9)$$

such that it approaches its limiting values exponentially in time, while it is again diffusive for short times and approximately scales with  $\langle(\Delta R_E)^2\rangle \sim t^{1/2}$  for intermediate times [49].

Finally the mean square displacement of the *center of mass* of the polymer chain scales in equilibrium as

$$\langle(\Delta r)^2\rangle \sim t \quad (10)$$

which turns out to be a good approximation for all times.

In Fig. 5 we compare these well known mean-square displacements for a polymer chain in a thermal bath (insets) with those for a chain in a bacterial bath with  $\phi = 0.02$  at a self-propulsion strength  $Pe = 10$ . We observe for all three studied quantities the same short and long-time behaviour. For short time, this is simply a result of our Brownian model. For long times, it is expected that an active solvent can hardly be discriminated from a passive one on average. At intermediate time, however, different behaviour gets visible. First of all, the end-monomer mean-square displacement shows an acceleration at intermediate times resulting in a larger value for the exponent  $\gamma(t)$ , compare Figure 5(a) with its inset. This obviously has to do with the intruding bacteria which brings in more dynamics into the chain. This effect is less pronounced for the end-to-end dynamics (Fig. 5(b)) where the dynamical behaviour is qualitative similar to the passive case, see the inset in Fig. 5(b).

Conversely, for the center of mass motion, there is a strong amplification of the bacterial dragging effect on the chain. Clearly, even new intermediate ballistic scaling regime shows up here where the mean-square displacement scales as  $t^2$ , compare Fig. 5(c) with its inset. Again, this has to do with the fact that in this regime the active particles drag the whole chain with it. The ballistic regime typically ceases to exist when the particle decorrelates its orientation, i.e. its pulling or dragging force, which occurs on a time scale  $1/D_r$ . This has been studied in great detail for a single Brownian active particle [71–73]. The decorrelation time scale  $1/D_r$  is plotted as a reference in Fig. 5(c) and represents indeed a reasonable upper bound at which the ballistic regime ceases to exist. Finally, as a further extreme reference, we have

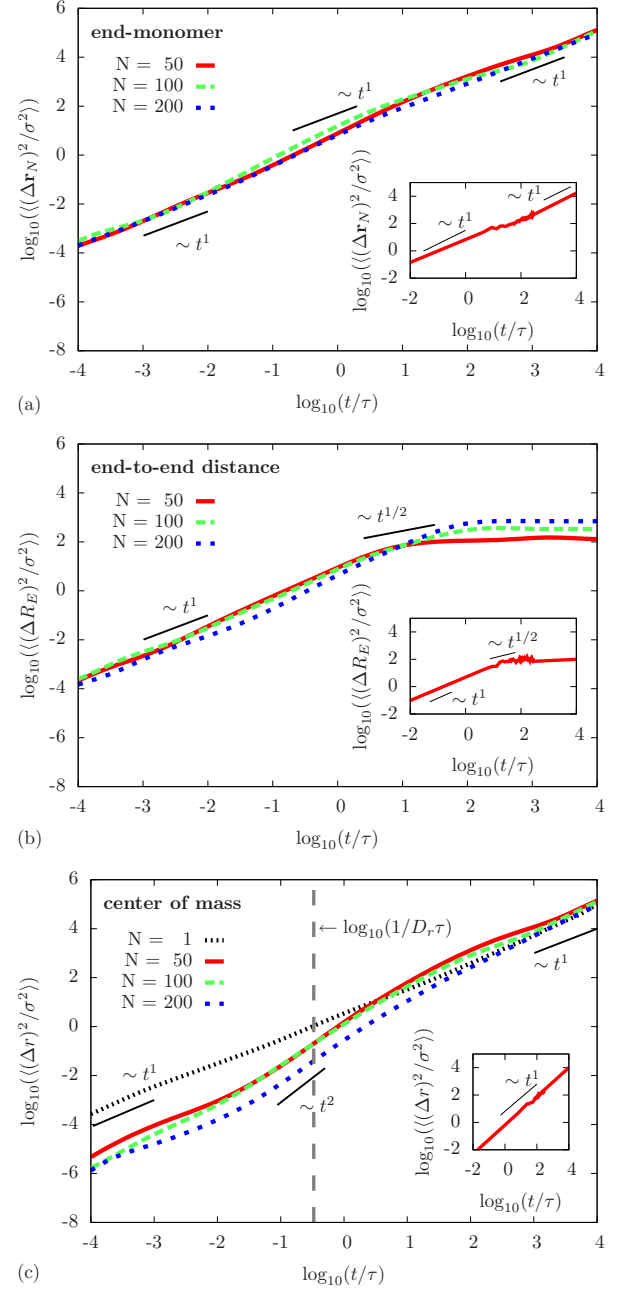


FIG. 5. Mean square displacements of (a) the *end-monomer*, (b) the *end-to-end distance*, and (c) the *center of mass* for various chain lengths  $N$  and a swimmer density of  $\phi = 0.02$  with self-propulsion strengths  $Pe = 10$ . The insets show the temporal behavior for a polymer in a pure thermal bath. The dashed vertical line in (c) indicates the rotational diffusion time scale  $1/D_r$  for an active swimmer.

included the case  $N = 1$  of a single segment, representing a passive tracer in a bath of active particles as studied recently [74, 75]. In this case, the ballistic regime is not very visible, since the collision time of active particles with the tracer is short.



## V. CONCLUSIONS

We have considered the impact of an active (bacterial) bath on the conformations of a flexible polymer chain in two dimensions by using extensive Brownian dynamics computer simulations. While the traditional Flory scaling for a two-dimensional self-avoiding random walk is found for large chains, there is an interesting nonuniversal behaviour for finite chain lengths. Due to the intruding bacteria, the polymer extensions are getting more stretched than predicted by Flory scaling and then crosses over to a plateau where the chain size does not depend on the molecular weight. This behaviour is unusual as it is not found in equilibrium. We have further identified trends of the chain size with increasing bacterial activity and find a relative compression for small activities and a strong stretching for large activities which we attribute to intrusion events of bacteria into the coiled chain. For the polymer dynamics, we find a  $t^2$  scaling for the center of mass mean square displacement for intermediate times, which is absent for an athermal solvent.

We hope that our findings will stimulate new explorations. First of all, a detailed theory would be challenging which predicts at least the scaling of the plateau behaviour. Moreover, more simulation will be necessary to understand the three-dimensional case both for one-dimensional chains where bacteria can more easily cir-

cumvent the polymer and for flexible membranes. In two dimensions our predictions can in principle be verified. Our model is best realized for colloidal polymers which are built by using lock-and-key colloids as monomeric entities [62]. These can easily be confined between glass plates and exposed to further artificial colloidal microswimmers such that the non-crossing situations which is crucial for our set-up is realized. It is less evident how our model is realized for real polymer chains and real bacteria as those are typical crossing in strong slit confinement. But a realistic set-up are bacteria close to a liquid-air interface which are standardly considered in experiments, see e.g. [56, 60, 61]. The latter interface is flexible but under tension. The intrusion effect, however, is also expected to play a leading role in case the line tension is small compared to thermal effects. Finally we think that the complex interaction between bacteria and flexible filaments as revealed in our study may be exploited in general for the fabrication of machines on the micro- and nanoscale [45].

## ACKNOWLEDGMENTS

We thank Berenike Maier, Roland Netz and Christian von Ferber for helpful discussions. This work was financially supported by the ERC Advanced Grant INTERCOCOS (Grant No. 267499) and by the SPP 1726 of the DFG.

- 
- [1] P. G. de Gennes, *Scaling concepts in polymer physics* (Cornell University Press, Ithaca, 1979).
  - [2] M. Doi and S. Edwards, *The Theory of Polymer Dynamics* (Clarendon Press, Oxford, 1986).
  - [3] L. Schäfer, *Excluded Volume Effects in Polymer Solutions: As Explained by the Renormalization Group* (Springer, 1999).
  - [4] A. Sokolov, I. S. Aranson, J. O. Kessler, and R. E. Goldstein, *Phys. Rev. Lett.* **98**, 158102 (2007).
  - [5] I. H. Riedel, K. Kruse, and J. Howard, *Science* **309**, 300 (2005).
  - [6] T. Vicsek and A. Zafeiris, *Phys. Rep.* **517**, 71 (2012).
  - [7] J. Zhang, W. Klingsch, A. Schadschneider, and A. Seyfried, *J. Stat. Mech.* **2012**, P02002 (2012).
  - [8] W. F. Paxton, A. Sen, and T. Mallouk, *Chem. Eur. J.* **11**, 6462 (2005).
  - [9] A. Snezhko and I. S. Aranson, *Nature Mat.* **10**, 698 (2011).
  - [10] F. Kümmel, B. ten Hagen, R. Wittkowski, I. Buttinoni, R. Eichhorn, G. Volpe, H. Löwen, and C. Bechinger, *Phys. Rev. Lett.* **110**, 198302 (2013).
  - [11] J. Palacci, C. Cottin-Bizonne, C. Ybert, and L. Bocquet, *Phys. Rev. Lett.* **105**, 088304 (2010).
  - [12] R. Dreyfus, J. Baudry, M. L. Roper, M. Fermigier, H. A. Stone, and J. Bibette, *Nature* **437**, 862 (2005).
  - [13] I. S. M. Khalil, H. C. Dijkslag, L. Abelmann, and S. Misra, *Appl. Phys. Lett.* **104**, 223701 (2014).
  - [14] M. N. Popescu, S. Dietrich, and G. Oshanin, *J. Chem. Phys.* **130**, 194702 (2009).
  - [15] S. Thakur and R. Kapral, *J. Chem. Phys.* **133**, 204505 (2010).
  - [16] G. Volpe, I. Buttinoni, D. Vogt, H.-J. Kümmerer, and C. Bechinger, *Soft Matter* **7**, 8810 (2011).
  - [17] J. Palacci, S. Sacanna, A. Vatchinsky, P. M. Chaikin, and D. J. Pine, *J. Am. Chem. Soc.* **135**, 15978 (2013).
  - [18] V. Narayan, S. Ramaswamy, and N. Menon, *Science* **317**, 105 (2007).
  - [19] X. Chen, X. Dong, A. Be'er, H. L. Swinney, and H. P. Zhang, *Phys. Rev. Lett.* **108**, 148101 (2012).
  - [20] A. M. Menzel and T. Ohta, *Europhys. Lett.* **99**, 58001 (2012).
  - [21] J. Gachelin, A. Rousselet, A. Lindner, and E. Clement, *New J. Phys.* **16**, 025003 (2014).
  - [22] S. Thutupalli, R. Seemann, and S. Herminghaus, *New J. Phys.* **13**, 073021 (2011).
  - [23] J. A. Cohen and R. Golestanian, *Phys. Rev. Lett.* **112**, 068302 (2014).
  - [24] H. H. Wensink, J. Dunkel, S. Heidenreich, K. Drescher, R. E. Goldstein, H. Löwen, and J. M. Yeomans, *Proc. Natl. Acad. Sci. USA* **109**, 14308 (2012).
  - [25] D. Saintillan and M. J. Shelley, *Phys. Fluids* **20**, 123304 (2008).
  - [26] S. Zhou, A. Sokolov, O. D. Lavrentovich, and I. S. Aranson, *Proc. Natl. Acad. Sci. USA* **111**, 1265 (2014).

- [27] K.-A. Liu and L. I, Phys. Rev. E **88**, 033004 (2013).
- [28] J. Palacci, S. Sacanna, A. P. Steinberg, D. J. Pine, and P. M. Chaikin, Science **339**, 936 (2013).
- [29] I. Buttinoni, J. Bialké, F. Kümmel, H. Löwen, C. Bechinger, and T. Speck, Phys. Rev. Lett. **110**, 238301 (2013).
- [30] G. S. Redner, M. F. Hagan, and A. Baskaran, Phys. Rev. Lett. **110**, 055701 (2013).
- [31] Y. Fily and M. C. Marchetti, Phys. Rev. Lett. **108**, 235702 (2012).
- [32] A. Zöttl and H. Stark, Phys. Rev. Lett. **112**, 118101 (2014).
- [33] S. K. Das, S. A. Egorov, B. Trefz, P. Virnau, and K. Binder, Phys. Rev. Lett. **112**, 198301 (2014).
- [34] H. H. Wensink and H. Löwen, Phys. Rev. E **78**, 031409 (2008).
- [35] M. B. Wan, C. J. Olson Reichhardt, Z. Nussinov, and C. Reichhardt, Phys. Rev. Lett. **101**, 018102 (2008).
- [36] I. Berdakin, Y. Jeyaram, V. V. Moshchalkov, L. Venken, S. Dierckx, S. J. Vanderleyden, A. V. Silhanek, C. A. Condat, and V. I. Marconi, Phys. Rev. E **87**, 052702 (2013).
- [37] J. Elgeti and G. Gompper, Europhys. Lett. **101**, 48003 (2013).
- [38] C. F. Lee, New J. Phys. **15**, 055007 (2013).
- [39] Y. Fily, A. Baskaran, and M. F. Hagan, arXiv preprint, arXiv:1402.5583 (2014).
- [40] P. Galajda, J. Keymer, P. Chaikin, and R. Austin, J. Bacteriol. **189**, 8704 (2007).
- [41] A. Guidobaldi, Y. Jeyaram, I. Berdakin, V. V. Moshchalkov, C. A. Condat, V. I. Marconi, L. Giojalas, and A. V. Silhanek, Phys. Rev. E **89**, 032720 (2014).
- [42] A. Kaiser, H. H. Wensink, and H. Löwen, Phys. Rev. Lett. **108**, 268307 (2012).
- [43] J. Tailleur and M. E. Cates, Europhys. Lett. **86**, 60002 (2009).
- [44] O. Chepizhko and F. Peruani, Phys. Rev. Lett. **111**, 160604 (2013).
- [45] L. Restrepo-Perez, L. Soler, C. S. Martinez-Cisneros, S. Sanchez, and O. G. Schmidt, Lab Chip **14**, 1515 (2014).
- [46] A. Kaiser, A. Peshkov, A. Sokolov, B. ten Hagen, H. Löwen, and I. S. Aranson, Phys. Rev. Lett. **112**, 158101 (2014).
- [47] A. Sokolov, M. M. Apodaca, B. A. Grzybowski, and I. S. Aranson, Proc. Natl. Acad. Sci. USA **107**, 969 (2010).
- [48] R. DiLeonardo, L. Angelani, D. DellArciprete, G. Ruocco, V. Iebba, S. Schippa, M. P. Conte, F. Mecarini, F. D. Angelis, and E. D. Fabrizio, Proc. Natl. Acad. Sci. USA **107**, 9541 (2010).
- [49] J. C. F. Schulz, L. Schmidt, R. B. Best, J. Dzubiella, and R. R. Netz, J. Am. Chem. Soc. **134**, 6273 (2012).
- [50] R. G. Winkler, Phys. Rev. Lett. **97**, 128301 (2006).
- [51] S. Liu, B. Ashok, and M. Muthukumar, Polymer **45**, 1383 (2004).
- [52] L. Cannavacciuolo, R. G. Winkler, and G. Gompper, Europhys. Lett. **83**, 34007 (2008).
- [53] A. Kaiser, K. Popowa, H. H. Wensink, and H. Löwen, Phys. Rev. E **88**, 022311 (2013).
- [54] L. Angelani and R. D. Leonardo, New J. Phys. **12**, 113017 (2010).
- [55] R. Ledesma-Aguilar and J. M. Yeomans, Phys. Rev. Lett. **111**, 138101 (2013).
- [56] S. Kjelleberg, B. A. Humphrey, and K. C. Marshall, Appl. Environ. Microbiol. **43**, 1166 (1982).
- [57] W. G. Pitt, M. O. McBride, A. J. Barton, and R. D. Sagers, Biomaterials **14**, 605 (1993).
- [58] C. Gómez-Suárez, H. J. Busscher, and H. C. van der Mei, Appl. Environ. Microbiol. **67**, 2531 (2001).
- [59] D. K. Powelson and A. L. Mills, Appl. Environ. Microbiol. **62**, 2593 (1996).
- [60] C. Meel, N. Kouzel, E. R. Oldewurtel, and B. Maier, Small **8**, 530 (2012).
- [61] A. Shklarsh, A. Finkelshtein, G. Ariel, O. Kalisman, C. Ingham, and E. Ben-Jacob, Interface Focus **2**, 689 (2012).
- [62] S. Sacanna, W. T. M. Irvine, P. M. Chaikin, and D. J. Pine, Nature **464**, 575 (2010).
- [63] W. Wang, W. Duan, A. Sen, and T. E. Mallouk, Proc. Natl. Acad. Sci. USA **110**, 17744 (2013).
- [64] I. Buttinoni, G. Volpe, F. Kümmel, G. Volpe, and C. Bechinger, J. Phys. Condens. Matter **24**, 284129 (2012).
- [65] D. Wu, K. Hui, and D. Chandler, J. Chem. Phys. **96**, 835 (1992).
- [66] K. Leung and D. Chandler, J. Chem. Phys. **102**, 1405 (1995).
- [67] K. Kremer and G. S. Grest, J. Chem. Phys. **92**, 5057 (1990).
- [68] H. H. Wensink and H. Löwen, J. Phys. Condens. Matter **24**, 464130 (2012).
- [69] J. Bialké, T. Speck, and H. Löwen, Phys. Rev. Lett. **108**, 168301 (2012).
- [70] M. Hinczewski, X. Schlagberger, M. Rubinstein, O. Krichevsky, and R. R. Netz, Macromolecules **42**, 860 (2009).
- [71] B. ten Hagen, S. van Teeffelen, and H. Löwen, J. Phys. Condens. Matter **23**, 194119 (2011).
- [72] J. R. Howse, R. A. L. Jones, A. J. Ryan, T. Gough, R. Vafabakhsh, and R. Golestanian, Phys. Rev. Lett. **99**, 048102 (2007).
- [73] X. Zheng, B. ten Hagen, A. Kaiser, M. Wu, H. Cui, Z. Silber-Li, and H. Löwen, Phys. Rev. E **88**, 032304 (2013).
- [74] K. C. Leptos, J. S. Guasto, J. P. Gollub, A. I. Pesci, and R. E. Goldstein, Phys. Rev. Lett. **103**, 198103 (2009).
- [75] G. Miño, J. Dunstan, A. Rousselet, E. Clement, and R. Soto, J. Fluid Mech. **729**, 423 (2013).